JOURNAL OF VIROLOGY, Aug. 2011, p. 7818–7827 Vol. 85, No. 15
0022-538X/11/$12.00 doi:10.1128/JVI.00325-11

The Requirement for Nucleoporin NUP153 during Human Immunodeficiency Virus Type 1 Infection Is Determined by the Viral Capsid[▽]

Kenneth A. Matreyek and Alan Engelman*

Department of Cancer Immunology and AIDS, Dana-Farber Cancer Institute, and Department of Medicine, Harvard Medical School, Boston, Massachusetts 02215

Received 16 February 2011/Accepted 10 May 2011

Lentiviruses likely infect nondividing cells by commandeering host nuclear transport factors to facilitate the passage of their preintegration complexes (PICs) through nuclear pore complexes (NPCs) within nuclear envelopes. Genome-wide small interfering RNA screens previously identified karyopherin β transportin-3 (TNPO3) and NPC component nucleoporin 153 (NUP153) as being important for infection by human immunodeficiency virus type 1 (HIV-1). The knockdown of either protein significantly inhibited HIV-1 infectivity, while infection by the gammaretrovirus Moloney murine leukemia virus (MLV) was unaffected. Here, we establish that primate lentiviruses are particularly sensitive to NUP153 knockdown and investigate HIV-1-encoded elements that contribute to this dependency. Mutants lacking functional Vpr or the central DNA flap remained sensitive to NUP153 depletion, while MLV/HIV-1 chimera viruses carrying MLV matrix, capsid, or integrase became less sensitive when the latter two elements were substituted. Two capsid missense mutant viruses, N74D and P90A, were largely insensitive to NUP153 depletion, as was wild-type HIV-1 when cyclophilin A was depleted simultaneously or when infection was conducted in the presence of cyclosporine A. The codepletion of NUP153 and TNPO3 yielded synergistic effects that outweighed those calculated based on individual knockdowns, indicating potential interdependent roles for these factors during HIV-1 infection. Quantitative PCR revealed normal levels of late reverse transcripts, a moderate reduction of 2-long terminal repeat (2-LTR) circles, and a relatively large reduction in integrated proviruses upon NUP153 knockdown. These results suggest that capsid, likely by the qualities of its uncoating, determines whether HIV-1 requires cellular NUP153 for PIC nuclear import.

The early steps of the retroviral life cycle occur within the context of nucleoprotein complexes that are derived from the core of the infecting viral particle. The reverse transcriptase (RT) enzyme converts genomic RNA into linear double-stranded viral DNA (vDNA) within the confines of the reverse transcription complex (RTC) (19, 20). Soon thereafter, the integrase (IN) enzyme catalyzes its initial activity, 3′ processing, whereby each vDNA 3′ end is cleaved adjacent to the conserved dinucleotide sequence CpA. This marks the transition from the RTC to the preintegration complex (PIC), wherein IN catalyzes its second catalytic function, DNA strand transfer (8, 23). Concomitantly, the complexes undergo morphological transitions, such as the dissolution of the viral capsid (CA) core, as they traffic from the cellular periphery to desired regions of host DNA within the nucleus (19, 20, 33, 51). Well-studied but still-unresolved aspects of these steps are the mechanisms by which retroviruses bypass the nuclear envelope, which physically separates the nuclear and cytoplasmic compartments of the cell (reviewed in reference 66). Although certain viruses, such as the gammaretrovirus Moloney murine leukemia virus (MLV), are believed to require the dissolution of the nuclear membrane during mitosis (61), lentiviruses such as human immunodeficiency virus type 1 (HIV-1) are able to infect nondividing cells and thus are believed to traverse the nuclear membrane by passing through the nuclear pore complex (NPC) (35, 42). As the HIV-1 PIC has been estimated to have a stokes radius of 28 nm (52) and thus grossly exceeds the ~9-nm diffusion limit (50) of the NPC, lentiviruses theoretically possess at least one mechanism to hijack the nuclear transport machinery and actively transport their PICs through the pore.

A number of HIV-1 PIC components, including matrix (MA), Vpr, IN, and the central DNA flap formed during reverse transcription, have been proposed to function during nuclear import, although significant roles for any of these components during this step have not been well corroborated. This may, at least in part, be reflective of redundant PIC nuclear import mechanisms, although viruses with these elements mutated in combination did not exhibit obvious cell cycle-dependent infectivity or nuclear import defects (60, 76). In contrast, CA can determine the ability of HIV-1 to infect nondividing cells, suggesting that viral core uncoating is a rate-limiting step of lentiviral PIC nuclear import (77, 78).

Numerous studies also have examined the requirements for specific cellular proteins during lentiviral/HIV-1 PIC nuclear import, including nuclear transport proteins NUP98 (17), importin 7 (81), karyopherin α2 Rch1 (24), and importin α3 (1). A series of three genome-wide short interfering RNA (siRNA) screens (7, 39, 84) highlighted nuclear transport proteins whose depletion strongly inhibited the early steps of HIV-1

* Corresponding author. Mailing address: Department of Cancer Immunology and AIDS, Dana-Farber Cancer Institute, 450 Brookline Avenue, CLS-1010, Boston, MA 02215. Phone: (617) 632-4361. Fax: (617) 632-4338. E-mail: alan_engelman@dfci.harvard.edu.

▽ Published ahead of print on 18 May 2011.

infection. This included transportin-3 (TNPO3) or transportin-SR2, a member of the karyopherin β superfamily responsible for transporting splicing factors with SR motifs into the nucleus. The depletion of TNPO3 resulted in a sizable HIV-1 nuclear import defect (13) while infection by MLV or the lentivirus feline immunodeficiency virus (FIV) remained largely unaffected (40, 41, 67), suggesting TNPO3 dependence to be specific to, although perhaps not obligatorily required by, lentiviruses. The mechanism by which HIV-1 physically hijacks TNPO3 remains unsolved; even though TNPO3 can bind HIV-1 IN (13), comparable levels of binding to MLV and FIV INs were observed (40, 67), and analyses of HIV-1 proteins relevant during the infection of TNPO3 knockdown cells implicated the CA protein as the genetic determinant of TNPO3 dependency (40).

In addition to TNPO3, two major constituent proteins of the NPC, nucleoporins NUP358/RanBP2 and NUP153, were identified in two of the siRNA screens (7, 39). NUP358 composes the large cytoplasmic filaments emanating from eukaryotic NPCs (74), the knockdown of which was recently confirmed to result in a defect of HIV-1 nuclear entry during infection (83). NUP153 is localized within the nucleus, linking central NPC scaffolding subcomplexes with their corresponding nuclear basket substructure, as well as anchoring individual NPCs with the nuclear lamina (71). Additionally, NUP153 dynamically shuttles between NPC-localized and nucleoplasmic populations (59). Although NUP153 knockdown also was interpreted to result in a defect in HIV-1 nuclear import, the lack of clear correlation between an approximately 85% reduction in acute infection and 20% reduction in 2-long terminal repeat (2-LTR)-containing DNA circle levels, a marker for PIC entry into the nucleus (39), suggested to us that other factors were at play. NUP153 has been reported to bind HIV-1 IN and Vpr (70, 73), suggesting potential mechanistic clues for the role of this host factor during HIV-1 infection. To investigate how NUP153 facilitates HIV-1 infection, we analyzed viral determinants that render HIV-1 sensitive to NUP153 depletion and additionally performed quantitative PCR (qPCR) analyses of the viral DNA species formed during the infection of NUP153 knockdown cells.

MATERIALS AND METHODS

Plasmid constructs. Infection assays utilized single-round viruses carrying either green fluorescent protein (GFP) or luciferase reporter genes. GFP-based constructs included equine infectious anemia virus (EIAV) (56, 57), HIV-1 (31), Rous sarcoma virus (RSV) (12) (Addgene plasmid 13878; obtained from Constance Cepko via Addgene, Cambridge, MA), FIV (36, 46), MLV (58, 68), Mason-Pfizer monkey virus (MPMV) (55), HIV-2 strain ROD (HIV-2_{ROD}), and simian immunodeficiency viruses from *Macaca mulatta* (SIV_{MAC}), *Chlorocebus sabaeus* (SIV_{AGM}Sab), and *Chlorocebus tantalus* (SIV_{AGM}Tan) (82). Luciferase-based viruses included MLV/HIV-1_{LAI} chimeras (75, 76) and HIV-1_{NL4-3}-derived D64N/D116N (N/N) IN active site and Vpr and/or DNA flap mutants of pNLX.Luc (45, 47). Vesicular stomatitis virus G (VSV-G) and HIV-1_{NL4-3} glycoprotein expression vectors were described previously (45, 47).

HIV-1 CA mutations were generated through the site-directed mutagenesis of the HIV-1_{NL4-3}-based pHP-dI-N/A packaging plasmid (10) (AIDS Research and Reference Reagent Program [ARRRP], Germantown, MD), which was cotransfected in conjunction with either pHI-vec2.GFP (32) or pHI-Luc (54) transfer vector. Sequencing was used to verify PCR-mutated DNAs. The NUP153 expression vector pIRES-dsRedExpress-NUP153 was created by digesting pCMV-Sport6-NUP153 (Open Biosystems, Huntsville, AL) with SalI and BglII and ligating the resulting NUP153 coding fragment with SalI/BamHI-digested pIRES-dsRedExpress (Clontech Laboratories, Mountain View, CA).

Cells and siRNA transfections. HEK293T and HeLa cells were cultured in Dulbecco's modified Eagle's medium supplemented to contain 10% fetal bovine serum, 100 IU/ml penicillin, and 100 μg/ml streptomycin, while GHOST cells expressing CD4 and the CXCR4 coreceptor (GHOST-CXCR4) (53) (ARRRP) additionally were cultured with 500 μg/ml G418, 100 μg/ml hygromycin, and 1 μg/ml puromycin. Approximately 75,000 HEK293T or 25,000 HeLa or GHOST-CXCR4 cells seeded per well of a 24-well plate were transfected the next day with a final concentration of 40 nM siNUP153#1 (GGACTTGTTAGATCTAGTT) (48), 10 nM siNUP153#2 (AGTGTTCAGTATGCTGTGTTTCT) (27), or 40 nM mismatch control of siNUP153#1, referred to as siControl ([GGTCTTATTGGA GCTAATT; underlines indicate base mismatches with siNUP153#1]) (Dharmacon, Lafayette, CO) using RNAiMax (Invitrogen, Carlsbad, CA) according to the manufacturer's instructions. Simultaneous NUP153 and cyclophilin A (CypA) knockdown was performed by transfection with a final concentration of 20 nM siNUP153#1, 20 nM CypA siRNA (AAGGGTTCCTGCTTTCACAGA) (11), or the corresponding amount of siControl for a total siRNA concentration of 40 nM. Simultaneous NUP153 and TNPO3 knockdown was performed similarly using siTNPO3 (CGACATTGCAGCTCGTGTA) (40). Medium was exchanged the following day. NUP153 reexpression was performed by $CaPO_4$ transfection of 1 μg DNA immediately after siRNA transfection.

Virus production. Vector particles were generated by transfecting HEK293T cells in 10-cm plates with a 10 μg total of various ratios of the aforementioned virus production plasmids using either $CaPO_4$ or Fugene 6 (Roche Molecular Biochemicals, Indianapolis, IN). The cells were washed 16 h after transfection, and supernatants collected 12 to 60 h thereafter were clarified at 300 × *g*, filtered through 0.45-μm filters (Nalgene, Rochester, NY), and either allotted and frozen or concentrated by ultracentrifugation using an SW28 rotor at 53,000 × *g* for 2 h at 4°C before freezing. Concentrations of Vpr, DNA flap, and CA mutant viral stocks were determined alongside concomitantly produced wild-type (WT) viruses using an exogenous ^{32}P-based RT assay (72).

Infectivity assays. Control and siRNA knockdown cells seeded onto 48-well plates were infected overnight with various reporter viruses 48 h after siRNA transfection. Percentages of GFP-positive cells were determined 36 h postinfection (hpi) using a FACSCanto flow cytometer (BD, Franklin Lakes, NJ) equipped with FACSDIVA software. GFP reporter experiments were performed with virus inoculates adjusted to yield <40% GFP-positive cells in control samples. Cells were infected with equal RT counts per minute (RTcpm) of WT or mutant HIV-1 luciferase reporter virus, while MLV/HIV-1 chimera viruses were adjusted such that all infections were within approximately 2 log relative light units (RLU)/μg/s of control cells. Where applicable, cyclosporine (Sigma, St. Louis, MO) was added at the time of infection to a final concentration of 5 μM. Cells infected with luciferase reporter viruses were lysed 48 hpi unless otherwise noted, and resulting levels of luciferase activity were normalized to the corresponding levels of total protein in cell extracts as described previously (40).

Normalized infectivity data were log transformed, and statistical analyses were performed by paired two-tailed Student's *t* test. Mean infectivity values then were back transformed for graphical representation, with error bars denoting 95% confidence intervals.

Western blot analysis. At the time of infection, siRNA-treated cells were lysed with radioimmunoprecipitation assay buffer (20 mM HEPES [pH 7.5], 150 mM NaCl, 1% NP-40, 1% sodium deoxycholate, 0.1% sodium dodecyl sulfate, 2 mM EDTA, Complete protease inhibitor [Roche Molecular Biochemicals]). Following the determination of protein concentration by Bradford assay, 60 μg or 2-fold dilutions of each lysate were fractionated through 9% Tris-glycine gels, and proteins were transferred onto a polyvinylidene fluoride membrane. NUP153 and NUP62 were detected using a 1:2,500 dilution of mouse mAb414 antibody (Abcam Inc., Cambridge, MA), while TNPO3 was detected using a 1:150 dilution of mouse anti-TNPO3 antibody ab54353 (Abcam Inc.). A 1:5,000 dilution of rabbit anti-mouse horseradish peroxidase-conjugated antibody served as the secondary antibody (Dako North America, Inc., Carpinteria, CA), and a 1:5,000 dilution of mouse anti-α-tubulin antibody (Abcam Inc.) was used as a loading control. Blots were developed using the ECL Plus detection reagent (GE Healthcare, Waukesha, WI).

qPCR. NUP153#1 or siControl-transfected cells (500,000) were infected with ~2 × 10^7 RTcpm of DNase-treated WT or N/N mutant virus, with parallel infections conducted in the presence 100 μM azidothymidine (AZT) (ARRRP) to define residual plasmid DNA levels potentially carried over from transfection. Two hours later, infected cells washed with phosphate-buffered saline were replated into individual 24-well plates. Cells were collected at various time points, and DNA was extracted with a QIAamp DNA Minikit as recommended by the manufacturer (Qiagen, Valencia, CA). Each sample was analyzed in triplicate by qPCR to determine levels of HIV-1 late reverse transcription (LRT), 2-LTR-containing circles, and integrated proviruses via nested Alu-PCR

essentially as described previously (9, 18). LRT and 2-LTR circle values were normalized to qPCR values for β-globin DNA performed in parallel, while all input DNAs for first-round Alu-PCRs were adjusted for equal β-globin amplification. Values obtained from corresponding AZT-treated samples, which averaged 2.6% of peak LRT and 2.5% of peak 2-LTR circles, were subtracted from nondrug-treated values.

Plasmid pNLX.luc.R− was used to generate LRT standard curves, while pUC19.2LTR was used for 2-LTR circles (47). The integration standard was prepared by infecting HeLa cells at relatively low multiplicities of infection with the pHI-puro transfer vector (54) and passaged for 2 weeks in 2 μg/ml puromycin to permit the loss of unintegrated HIV-1 DNA forms, and total DNA was extracted using the QIAamp DNA Minikit. Twofold dilutions of infected cell DNA were mixed with complementary amounts of DNA prepared from uninfected HeLa cells to form the standard curve. Twofold dilutions of uninfected cell DNA were used as the standard for β-globin.

qPCR primers and probes were the following: MH531, MH532, and MH535 for LRT (9) and 2-LTR circle junction (34); AE3014, AE1066, AE3013, AE990, and AE995 for Alu-PCR (15, 18); and β-globin+ and β-globin− for HeLa genomic DNA (79). SYBR green was used to measure β-globin amplification.

RESULTS

Depletion of NUP153 expression inhibits HIV-1 infection. RNA interference was used to knock down NUP153 expression and analyze the role of this host factor during HIV-1 infection. HeLa cells were transfected with one of two previously characterized NUP153-specific siRNAs (27, 48) or a nontargeting siControl mismatch to siNUP153#1, and protein expression levels were measured 48 h later. Semiquantitative Western blotting of whole-cell lysates showed NUP153 expression to be depleted greater than 8-fold by either siRNA (Fig. 1A). NUP153 knockdown cells infected with HIV-1 or MLV revealed that siNUP153#1 and siNUP153#2 significantly reduced HIV-1 infectivity to 3.2 and 3.4% of siControl-treated cells, respectively (Fig. 1B). MLV was less or not significantly inhibited in parallel infections. Because cells transfected with siNUP153#2 showed evidence of cytotoxicity (data not shown), siNUP153#1 was used for the remainder of the study.

To further address the specificity of NUP153 knockdown on HIV-1 infection, protein levels in depleted cells were restored via expression of an exogenously introduced siRNA-insensitive cDNA. siRNA-transfected HEK293T cells were retransfected with the inert pUC19 plasmid, an empty expression vector encoding an internal ribosome entry site (IRES)-controlled dsRed-Express fluorescent protein, or an engineered vector encoding NUP153 5′ of the IRES element. Western blot analysis of cells lysed at the time of infection showed more robust exogenous NUP153 expression than the endogenous protein in both knockdown and control cells (Fig. 1C). As gross overexpression of NUP153 has been shown to distort the nuclear envelope (5), virus-infected GFP-positive cells were quantitated within cell populations gated for the dim fluorescence of the dsRed-Express protein. HIV-1 infection of NUP153 knockdown HEK293T cells was significantly inhibited compared to the infection of control cells, while exogenous NUP153 expression restored infection to levels similar to those of controls (Fig. 1D). Although MLV in this experiment was partially affected by NUP153 knockdown, this effect was inert to NUP153 reexpression.

Differential retroviral dependencies on cellular NUP153. We investigated whether NUP153 dependency was specific or common to lentiviruses by testing the infectivities of a panel of retroviral reporter constructs. To determine whether the stark

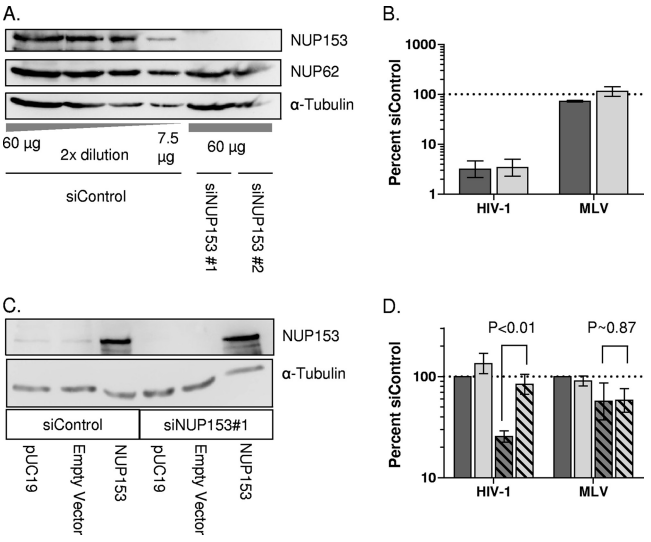

FIG. 1. NUP153 expression and HIV-1 infection. (A) Twofold dilutions of a whole-cell extract from control cells (lanes 1 to 4) compared to extracts from NUP153-depleted cells (lanes 5 and 6). NUP62 cross-reacted with the utilized anti-NUP153 antibody. (B) Percent infectivity of GFP reporter viruses in HeLa cells transfected with siNUP153#1 (dark gray) or siNUP153#2 (light gray) compared to control cells. Results are averages from three experiments, each performed in triplicate; error bars denote 95% confidence intervals. (C) HEK293T cells transfected with siControl or siNUP153#1 were retransfected with either control DNA (pUC19), empty IRES-dsRed-Express vector, or the vector expressing siRNA-resistant NUP153 protein. (D) Cells in panel C were gated for dim dsRed-Express expression, and the infectivities of GFP reporter viruses were normalized to those of cells transfected with the empty vector. Solid and hatched bars, cells transfected with siControl and siNUP153#1, respectively; dark and light gray bars, cells transfected with empty and NUP153 expression vectors, respectively. The results are averages from four experiments performed in duplicate, with error bars denoting 95% confidence intervals.

infectivity defect observed with HIV-1 extended to other primate lentiviruses, GFP reporter viruses for HIV-2_{ROD}, SIV_{MAC}, SIV_{AGM}Tan, and SIV_{AGM}Sab were analyzed. NUP153 depletion significantly inhibited infection by each of these viruses, with values ranging from 3.3% for SIV_{AGM}Tan to 10.6% for SIV_{MAC}, while infection by MLV was slightly enhanced under these conditions (Fig. 2A). In contrast, similar experiments showed more-divergent retroviruses to be less sensitive to NUP153 depletion (Fig. 2B). NUP153 knockdown significantly inhibited EIAV infection, to 33.4% of the level for the control. The alpharetrovirus RSV and betaretrovirus MPMV also were significantly affected but to even lesser extents, at 53.7 and 38.7% of the control level, respectively (Fig. 2B). Consistently with results of Lee et al. (41), infection by FIV was largely unaffected by NUP153 knockdown.

Neither Vpr nor the central DNA flap play significant roles in NUP153 dependency during HIV-1 infection. Viral elements implicated in HIV-1 nuclear import were analyzed to determine which ones might contribute to NUP153 dependency. Neither the central DNA flap nor Vpr are essential for HIV-1 infectivity, so mutations that completely abrogated function were analyzed here (22, 45). Reporter viruses with either or both elements mutated were applied to NUP153 or control

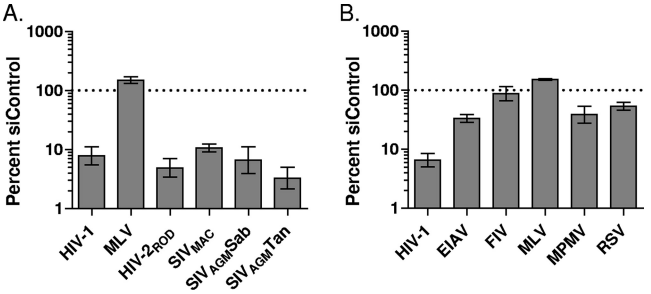

FIG. 2. Retroviral susceptibilities to NUP153 knockdown. HeLa cells transfected with siNUP153#1 or siControl were infected with GFP reporter viruses specific to primate lentiviruses (A) or different types of retroviruses (B). Results are averages from at least three experiments performed in triplicate, with error bars denoting 95% confidence intervals.

knockdown cells at two levels of input (5×10^6 or 5×10^4 RTcpm). Similarly to previous observations, single and double mutant viral infectivities were comparable to that of the WT (22, 45, 60) (Fig. 3A, dark gray bars). To determine whether sensitivity to NUP153 depletion was altered by these mutations, the infectivities of each mutant virus in knockdown cells were normalized to their corresponding control sample and regraphed (Fig. 3B). Infections performed with either quantity of viral inocula were significantly decreased when NUP153 was knocked down, although as a group infections performed with less virus showed a slight, but not significant, increase in sensitivity to the knockdown. Although Vpr mutant viruses showed slight differences in sensitivity to the knockdown with both quantities of inocula, none of these values reached statistical significance.

Replacement of HIV-1 IN or CA with MLV counterparts influences NUP153 dependency, while MA does not. Essential roles of MA, IN, and CA proteins during the early and/or late steps of HIV-1 replication precluded the use of deletion constructs in infectivity assays. Because NUP153 depletion resulted in dramatically different levels of MLV and HIV-1 infection (39) (Fig. 1B), we instead tested a set of HIV-1-based chimera viruses containing differing amounts of MLV Gag

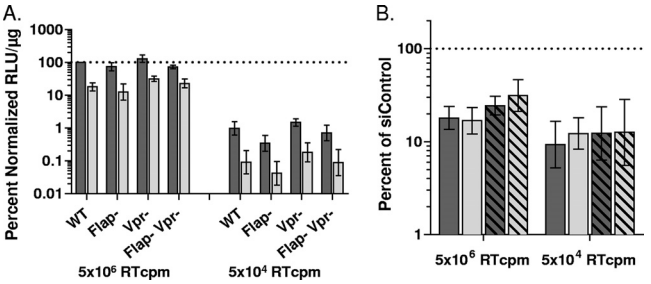

FIG. 3. NUP153 dependency during HIV-1 infection is independent of Vpr and the central DNA flap. (A) Viral infectivities were normalized to the level obtained with 5×10^6 RTcpm of WT virus (set to 100%). Dark gray, siControl; light gray, siNUP153#1. (B) Regraph of panel A results, with infectivities in knockdown cells expressed as percentages of control cells, which were set at 100%. Solid dark gray, WT virus; light gray, DNA flap mutant; hatched bars, Vpr mutant viruses. Results are averages from four experiments performed in duplicate, with error bars denoting 95% confidence intervals.

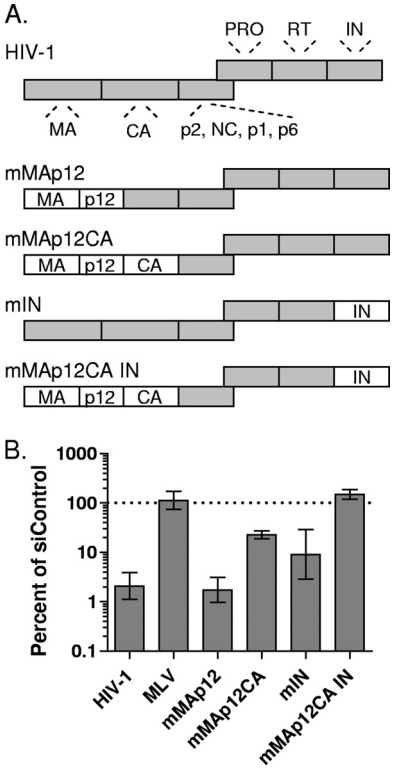

FIG. 4. NUP153 dependencies of MLV/HIV-1 chimera viruses. (A) Illustration of constructs tested (not to scale), with major HIV-1 Gag and Pol proteins indicated in gray (NC, nucleocapsid; PR, protease) and MLV proteins in white. (B) Control or knockdown cells were infected with HIV-1_{LAI}, MLV, or HIV-1-derived MLV chimera viruses shown in panel A. Results are averages from three experiments performed in triplicate, with error bars denoting 95% confidence intervals.

and/or Pol proteins (75, 76) (Fig. 4A). Chimera viral names indicate the swapped MLV protein(s). For example, mMAp12 carries MLV MA and p12, whereas mMAp12CA additionally harbors MLV CA.

Upon NUP153 depletion, the infectivity of the parental HIV-1_{LAI} isolate was significantly decreased to 2.1% of that of the control, while MLV remained unaffected at 112.1% (Fig. 4B). The infectivity of mMAp12 was indistinguishable from that of HIV-1_{LAI}, while the addition of MLV CA reduced dependency on NUP153 about 10-fold, to 22.7% of that of the control. The separate replacement of the IN protein in mIN also yielded a significant, approximately 4-fold difference from HIV-1_{LAI} to 9.1% of that of the control, although this sample exhibited greater experimental variability. The combination virus containing MLV MA, p12, CA, and IN was not inhibited by NUP153 depletion, exhibiting 149.6% infectivity compared to that of the control.

Alteration of HIV-1 sensitivity to NUP153 depletion by CA missense mutations or cyclosporine treatment. The preceding experiment revealed CA as a dominant determinant of NUP153 dependency, so we next surveyed a panel of previously characterized CA missense mutant viruses for NUP153 dependency during infection. Mutants of the cyclophilin A (CypA) binding loop, encompassing HIV-1 residues His83 to

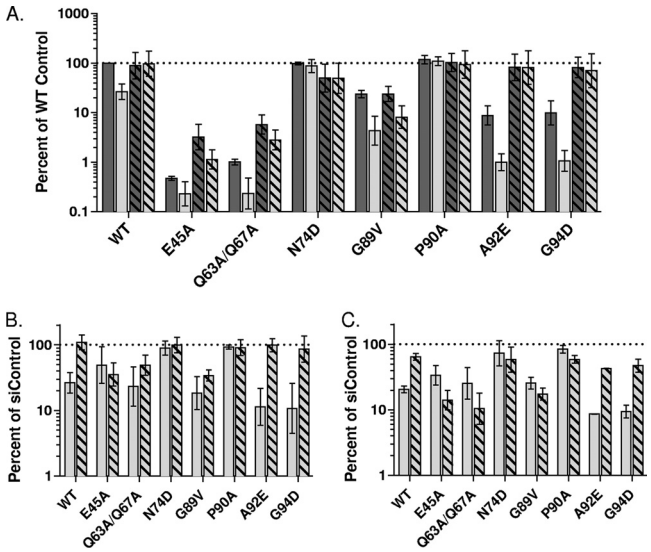

FIG. 5. WT and CA mutant viral infectivities and cyclosporine dependences in control and NUP153 knockdown cells. (A) Control (dark gray) or NUP153 knockdown (light gray) cells were left untreated (solid bars) or were treated with 5 μM cyclosporine (hatched bars) at the time of infection. All samples were normalized to the infectivity of WT virus in untreated control cells, which was set at 100%. The results are averages from three experiments, each performed in duplicate, with error bars denoting 95% confidence intervals. (B) Regraph of panel A results, with infectivities in knockdown cells expressed as percentages of the infectivity of control cells; hatched bars denote infections in the presence of CsA. The results are averages from six experiments performed in duplicate, with error bars denoting 95% confidence intervals. (C) Infectivities in NUP153 knockdown cells compared to that of control cells, with hatched bars denoting cells in which CypA was simultaneously depleted. Results are averages from two experiments performed in duplicate, with error bars denoting 95% confidence intervals.

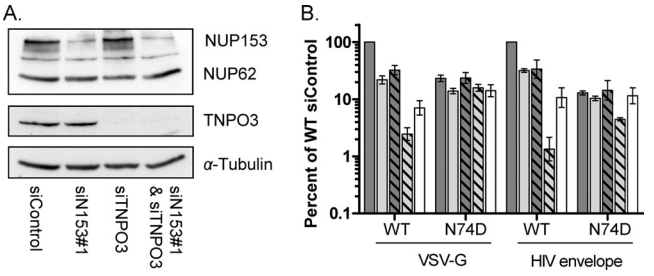

FIG. 6. Interdependence of NUP153 and TNPO3 during HIV-1 infection. (A) Whole-cell extracts of control, NUP153-depleted, TNPO3-depleted, and combinatorially depleted cells were blotted with the indicated primary antibodies. (B) Control (dark gray) or NUP153 knockdown (light gray) cells simultaneously depleted for TNPO3 (hatched bars) were infected with 2×10^6 or 2×10^7 RTcpm of VSV-G or HIV-1 envelope pseudotyped viruses, respectively, yielding numbers of RLU in control cells that were within 1 log of each other (not shown). All samples were normalized to the infectivity of the WT virus in control cells, which was set at 100%. White bars show the multiplicative product of infectivity defects exhibited upon individual protein knockdowns, representing the theoretical maximum expected assuming independent function. Results are averages from three experiments, each performed in duplicate, with error bars denoting 95% confidence intervals.

Arg99, included G89V and P90A, which exhibit greatly diminished CypA binding (80), and A92E and G94D, whose infectivities are cell type specific (29, 65). Non-CypA loop mutants E45A and Q63A/Q67A, which exhibit altered core stability both *in vitro* and *ex vivo* (16, 21, 25, 78), experience greatly decreased infectivities across cell types. A relatively large viral inoculum, 4×10^6 RTcpm, therefore was utilized to provide robust signals across the mutant virus set.

Consistently with previous reports, the infectivities of E45A and Q63A/Q67A were severely compromised, while G89V, A92E, and G94D yielded moderate defects and the N74D and P90A mutants infected HeLa cells at levels comparable to that of the WT (Fig. 5A, dark gray bars). Comparison of infectivities in knockdown and control cells confirmed N74D to be insensitive to NUP153 depletion (41) (Fig. 5A and B, light gray bars). E45A appeared moderately less sensitive to knockdown than the WT, while the Q63A/Q67A mutant was not distinguishable from the WT. A92E and G94D were at least as, if not more, sensitive to NUP153 depletion as the WT, while the CypA binding mutants G89V and P90A exhibited contrasting sensitivities: G89V was sensitive while P90A was resistant (Fig. 5A and B, light gray bars). The P90A phenotype appeared to be cell type specific, as partial sensitivity to NUP153 knockdown was observed in HEK293T and GHOST-CXCR4 cells (data not shown).

As the interaction of CA with CypA can govern HIV-1 uncoating (44), WT and CA mutant viral dependencies were evaluated in the presence of cyclosporine to disrupt this protein-protein interaction. As previously observed in HeLa cells (29, 64), the WT was relatively unaffected by cyclosporine treatment, while E45A, Q63A/Q67A, A92E, and G94D witnessed approximately 5- to 10-fold increases in infectivity (Fig. 5A, compare dark gray hatched and solid bars). Interestingly, cyclosporine treatment rendered the WT, A92E, and G94D viruses fully insensitive to NUP153 depletion (Fig. 5A, dark gray hatched bars, and B, hatched bars). This effect was not observed with all NUP153-sensitive CA mutants, as the G89V mutant remained largely dependent on the host factor in the presence of the drug. Similar results were observed with CypA knockdown in place of cyclosporine treatment: CypA knockdown resulted in approximately 5- to 20-fold increases in the infectivities of E45A, Q63A/Q67A, A92E, and G94D mutant viruses (data not shown), and WT, A92E, and G94D viruses were rendered significantly less sensitive to NUP153 depletion when CypA was knocked down simultaneously (Fig. 5C, compare hatched to solid bars).

Interdependent requirement for NUP153 and TNPO3 during HIV-1 infection. Primate lentiviruses reveal strong dependencies on NUP153 and TNPO3, while MLV, FIV, and the N74D HIV-1 CA mutant are largely unaffected by either knockdown (40, 41) (Fig. 2). We therefore next tested if these proteins would reveal evidence for interdependence during HIV-1 infection. Because Thys et al. (67) recently showed that the route of N74D entry influenced the requirement for TNPO3, experiments were conducted in CD4-positive GHOST-CXCR4 cells to enable comparisons of VSV-G and HIV-1 envelope pseudotyped particles. NUP153 and TNPO3 were knocked down either individually or in combination (Fig. 6A). WT viruses carrying either envelope exhibited 3- to 5-fold decreases in infectivity when NUP153 (Fig. 6B, light gray bars) or TNPO3 (dark gray hatched bars) was knocked down, while

N74D was largely, if not completely, insensitive. Interestingly, a 40-fold decrease in infection by VSV-G-pseudotyped WT virus was observed when both proteins were knocked down (Fig. 6B, light gray hatched bar), far greater than the ~14-fold defect expected based on the product of individual knockdowns (Fig. 6B, white bar). The N74D mutant showed no such effect, with the dual knockdown inhibiting this virus no more than the slight decrease observed with NUP153 knockdown alone. The results with the HIV-1 envelope pseudotypes were similar, although slightly exaggerated: WT virus exhibited an approximately 75-fold infection defect when both factors were knocked down, while the N74D mutant exhibited a much smaller, though noticeable, 3-fold decrease in infectivity.

NUP153 depletion inhibits expression from an integration-defective reporter virus. HIV-1 reporter viruses harboring mutations of IN active-site residues are unable to catalyze vDNA integration but still can yield a reproducible level of reporter gene expression. N/N active-site mutant viruses carrying either WT or N74D CA therefore were produced to determine if the inhibitory effects of NUP153 depletion were conferred in the absence of integration. Infection with N/N mutant viruses yielded ~2 to 3% reporter expression compared to that of the WT IN viruses, and as expected, these gene expression levels were completely refractory to the addition of 10 μM strand transfer inhibitor raltegravir, a dose ~100-fold in excess of that required to inhibit 95% of WT viral infection (38) (Fig. 7A). Control and NUP153 knockdown cells next were challenged with N/N viruses alongside 10-fold dilutions of WT IN viruses to establish a comparable level of endpoint reporter expression (Fig. 7B). The N/N virus harboring WT CA was significantly inhibited by NUP153 depletion to a level indistinguishable from that of its integration-competent counterpart at all viral inocula tested (Fig. 7C). Additionally, similarly to the effects of the N74D change on integrating virus, the N74D CA mutation rendered the N/N virus insensitive to NUP153 depletion.

NUP153 depletion results in decreased 2-LTR circles and integrated proviruses. Although NUP153 depletion previously was concluded to result in an HIV-1 PIC nuclear import defect, this interpretation was based on an approximately 20% reduction in 2-LTR circle levels at 24 hpi alongside an 8-fold infectivity defect (39). To more comprehensively address the block to HIV-1 infection upon NUP153 depletion, LRT, 2-LTR circle, and integrated proviral DNA levels were measured at multiple time points by qPCR following infection with either WT or N/N mutant virus. As expected (30), cells infected with N/N virus supported a level of LRT products similar to that of WT-infected cells at 8 hpi, with a corresponding ~9.6 fold increase in 2-LTR circle levels at 24 hpi (data not shown). WT and N/N mutant viral reverse transcription were insensitive to the amount of cellular NUP153, as peak levels at 8 hpi were similar in control and knockdown cells (Fig. 8A and D). NUP153 depletion resulted in an approximately 4.7-fold decrease in N/N virus 2-LTR circle formation at 24 hpi, which leveled off somewhat, to 3.2-fold, by 52 hpi (Fig. 8E). In contrast, NUP153-depleted cells infected with WT virus supported 2.1- and 2.3-fold lower 2-LTR circle levels than siControl-transfected cells at 24 and 52 hpi, respectively (Fig. 8B). WT viral integration was blocked more significantly than 2-LTR circles in NUP153 knockdown cells, about 5- and 7.2-fold lower than the levels of integrated proviruses in control cells at 24 and 52 hpi, respectively (Fig. 8C). Comparison of luciferase activities at 52 hpi yielded approximately 9.3- and 10.7-fold reductions in WT and N/N mutant viral infectivities, respectively, upon NUP153 knockdown (Fig. 8F).

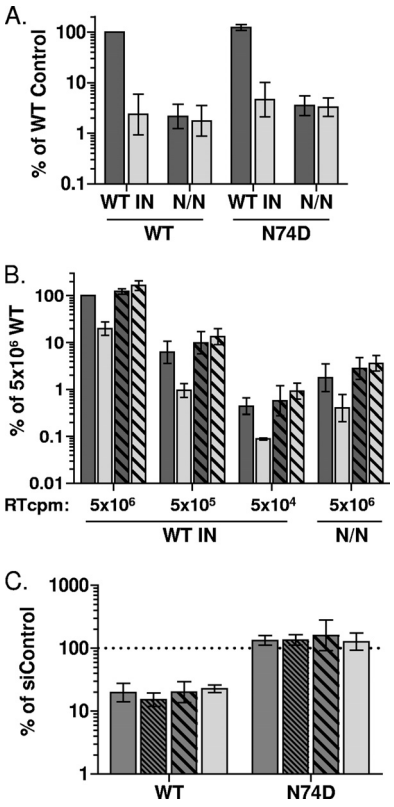

FIG. 7. NUP153 dependencies of WT and IN active-site mutant viruses. (A) Relative differences in reporter expression of 5×10^6 RTcpm WT and N/N IN mutant, along with WT sequence or the CA N74D mutation, in the absence (dark gray) or presence (light gray) of 10 μM raltegravir. (B) Relative infectivities of WT and N/N mutant viruses in control (dark gray) or NUP153 knockdown cells (light gray), with WT infectivity (5×10^6 RTcpm) set to 100%. Viruses harbored either WT (solid bars) or N74D (hatched bars) CA. (C) Regraph of panel B results, with infectivities in knockdown cells expressed as percentages of respective control cells; solid, hatched, and boldface hatched bars denote infections with 5×10^6, 5×10^5, and 5×10^4 RTcpm of WT IN virus, respectively, while light gray bars denote infection with N/N virus. Results are averages from five experiments performed in triplicate, with error bars denoting 95% confidence intervals.

DISCUSSION

NUP153 is likely required for HIV-1 nuclear entry. NUP153 expression has been shown to be required for HIV-1 infection (7, 39), but its role(s) in this process has yet to be well characterized. Here, we show that NUP153 is required for efficient infection by primate lentiviruses and may play a role in infection by other retroviral genera (Fig. 2). Our results with integration-defective N/N virus revealed NUP153 to be equally required for expression from integrated and unintegrated vDNA templates, implicating a step common to both processes. Our investigations tracking viral DNA accumulation in NUP153-depleted cells showed both WT and N/N IN mutant

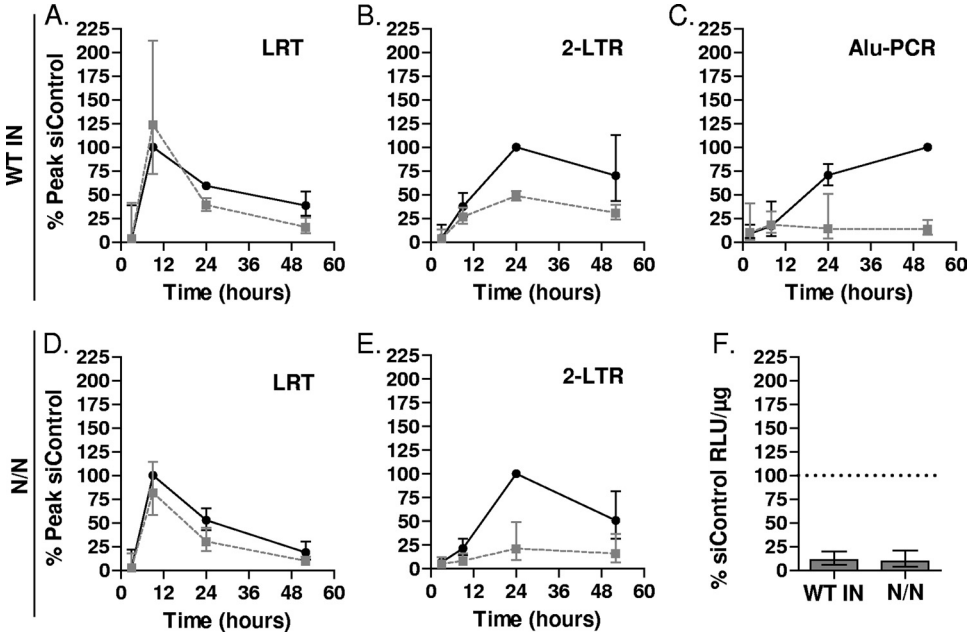

FIG. 8. HIV-1 DNA species formed during acute infection of NUP153 knockdown cells. Viral DNAs were amplified from cells following infection with WT (A, B, and C) or N/N mutant (D and E) virus, with values from NUP153 knockdown cells (gray dashed line) normalized to peak LRT (8 hpi) (A and D), 2-LTR circle (24 hpi) (B and E), and integration (52 hpi) (C) values. (F) Levels of WT and N/N mutant virus infectivities upon NUP153 depletion, expressed as percent siControl-transfected cells (set at 100%). Results are averages from three experiments, with error bars denoting 95% confidence intervals.

viral LRT levels similar to those of control cells, suggesting that NUP153 expression is not necessary for reverse transcription. In contrast, knockdown cells infected with the N/N mutant supported formation of about 5-fold fewer 2-LTR circles than NUP153-expressing cells (Fig. 8). The nonhomologous end-joining machinery required for 2-LTR circle formation is expected to reside in the nucleus (26, 43), which suggests that NUP153 is involved at a step(s) following reverse transcription which could precede or coincide with nuclear entry or a subsequent process that facilitates the formation and/or retention of 2-LTR circles. Because NUP153 is an NPC component, it seems most likely that the defect is at nuclear entry. Accordingly, knockdown cells infected with WT virus exhibited decreased levels of 2-LTR circles as well, albeit to a lesser extent than the N/N mutant. This discrepancy may be due to an overlying integration defect, which would be expected to contribute to the accumulation of vDNAs susceptible to circularization.

CA mutant viruses and cyclosporine treatment indicate a role for core uncoating in NUP153 dependency during HIV-1 infection. Although the infection defect likely is at a nuclear step, the major functional determinant of NUP153 dependency identified thus far appears to be the CA protein (41) (Fig. 4 to 6). It is possible that CA molecules associated with the PIC directly participate in steps at the NPC or within the nucleus, but because numerous point mutations across different faces of the HIV-1 CA monomer can dramatically alter NUP153 dependence, it is more likely that the dominant effects of CA are reflective of qualities conferred by a multimerized CA core. These results suggest that NUP153 dependency is an effect dictated by the manner in which the CA core uncoats in the cytoplasm or potentially at the nuclear pore itself (2). Consistent with this interpretation, we found that the perturbation of cyclophilin binding, either by cyclosporine treatment or CypA knockdown, dictated the sensitivity of the WT and cyclosporine-dependent mutants A92E and G94D to NUP153 depletion (Fig. 5). Thus, it appears as though the amount of CypA bound to the HIV-1 core is able to dictate whether the PIC undergoes downstream processes requiring NUP153, perhaps by altering the dynamics of uncoating (44). Notably, this level of regulation by CypA does not appear to be a global requisite for infection, as SIV_{MAC} is highly sensitive to NUP153 knockdown in spite of its reported inability to bind CypA (6). The route of cell entry taken by the N74D CA mutant, which has been documented to alter the requirement for TNPO3 during infection (67), may influence NUP153 dependency as well. Although the HIV-1-mediated entry of N74D failed to reveal a requirement for NUP153 or TNPO3 in our hands, we did note a modest 3-fold effect upon the depletion of both proteins (Fig. 6).

Notably, there is precedence for a requirement of NUP153 and NUP153-like proteins during infection with other viruses and retrotransposons at a stage that interfaces capsid oligomerization with nuclear import. The *Saccharomyces pombe* ortholog Nup124p is important for the nuclear accumulation of the Tf1 retrotransposon (3, 14). Interestingly, residues adjacent to an N-terminal nuclear localization signal located in Tf1 Gag dictated whether Nup124p was necessary for Gag nuclear import, and this appeared to correlate with the ability of Gag to multimerize (37). More recently, NUP153 was found to play a key role during hepatitis B virus nuclear import by signaling mature capsid proteins to dissociate within the NPC basket

(63). Interestingly, both Tf1 Gag and hepatitis B virus capsid have been demonstrated to directly bind their respective NUP153 orthologs. It therefore would be instructive to know if human NUP153 binds HIV-1 CA in an oligomerization-dependent manner.

A potential role for IN in NUP153 dependency. Aside from the dominant effects conferred by CA, our functional studies of viral elements provide context to understand potential physical interactions relevant to NUP153 function during infection. Although NUP153 has been found to bind HIV-1 Vpr (70), viruses lacking virion-incorporated Vpr were not significantly altered in their NUP153 dependence compared to that of the WT virus, suggesting that this interaction is not relevant up to and including the nuclear import, integration, and early gene expression stages of infection (Fig. 3). NUP153 also has been found to bind HIV-1 IN (73), and our results with MLV/HIV-1 chimera viruses support a role for HIV-1 IN during the infection of NUP153 knockdown cells (Fig. 4). Additionally, the IN protein of FIV previously was found not to bind NUP153 (73), which appears to correlate with the insensitivity of this virus to NUP153 depletion (Fig. 2B). As yet, the requirement for IN appears auxiliary to CA: despite carrying WT IN, HIV-1 CA mutants N74D and P90A were largely insensitive to NUP153 knockdown (Fig. 5 and 6), while comparison between chimeras containing MLV IN or CA showed the replacement of CA to decrease the sensitivity of the virus to knockdown more than IN replacement (Fig. 4).

Pleiotropic effects of NUP153 depletion. It currently is unknown whether the effect of NUP153 knockdown on primate lentiviral infection is reliant on the cellular roles of NUP153 during nuclear transport or on other collateral pleiotropic effects caused by the depletion of this multifunctional protein. NUP153 is believed to be a major point of NPC interaction with translocating karyopherins, including those for nuclear import via importin α/β and transportin, protein export via Crm1, and mRNA export via NXF1 (reviewed in reference 4). Furthermore, NUP153 depletion has been shown to prevent the NPC from incorporating nucleoporins Tpr and NUP50 (28, 49), and it also has been shown to perturb NUP62, NUP88, and NUP214 localization in certain contexts (48, 62). Thus, even if the disruption of a putative specific HIV-1 PIC-NUP153 interaction(s) is not the root cause of the infectivity defect, it may be due to the mislocalization of a subsequently required, potentially unidentified host factor. Furthermore, NUP153 can exert effects indirectly of nuclear transport, as its depletion has been shown to disrupt the cytoskeleton (85), likely through the perturbation of the nuclear lamina, and it also has been found to delay cellular progression through mitosis (48, 49). Lastly, NUP153 is important during transcription and even has been found to be associated with large regions of transcriptionally active open chromosomes within the *Drosophila* genome (69). Regardless, although NUP153 depletion is known to disrupt many processes within the cell, its overall relevance to HIV-1 infection must be relatively specific, as single point mutations in CA can render the virus completely unaffected (Fig. 5).

It will be interesting to continue to determine the role of NUP153 in relation to other host factors implicated in HIV-1 nuclear transport, especially TNPO3 and NUP358. Numerous similarities have been observed upon the knockdown of individual components: HIV-1 exhibits a nuclear entry defect (13, 39, 83) (Fig. 8), while MLV, FIV, and the N74D CA mutant are seemingly unaffected (7, 13, 39–41, 67) (Fig. 2, 5, and 6). Here, we determined that the simultaneous depletion of NUP153 and TNPO3 significantly enhanced the block to HIV-1 infection, suggesting interrelated functions. Perhaps these proteins represent multiple components of a concerted mechanism streamlining the early steps of HIV-1 infection, allowing for both optimal quantity and quality of proviral insertion into the host genome.

ACKNOWLEDGMENTS

This study relied on the generous contributions of reagents from the following colleagues: Lung-Ji Chiang, Michael Emerman, Dana Gabuzda, Theodora Hatziioannou, Eric Hunter, Welkin Johnson, Richard Mulligan, John Olsen, Eric Poeschla, Joseph Sodroski, and Masahiro Yamashita. GHOST-CXCR4 cells were obtained from Vineet N. KewalRamani and Dan Littman through the ARRRP, Division of AIDS, NIAID, NIH.

This work was supported by National Institutes of Health grant AI052014 (A.E.) and the Harvard University Center for AIDS Research, an NIH-funded program (P30AI060354) that is supported by the following NIH institutes and centers: NIAID, NCI, NIMH, NIDA, NICHD, NHLBI, and NCCAM.

Results, data interpretation, and the mention of commercial reagent sources in no way reflect the opinions of or endorsement by the U.S. government.

REFERENCES

1. **Ao, Z., et al.** 2010. Importin alpha3 interacts with HIV-1 integrase and contributes to HIV-1 nuclear import and replication. J. Virol. **84:**8650–8663.
2. **Arhel, N. J., et al.** 2007. HIV-1 DNA Flap formation promotes uncoating of the pre-integration complex at the nuclear pore. EMBO J. **26:**3025–3037.
3. **Balasundaram, D., M. J. Benedik, M. Morphew, V. D. Dang, and H. L. Levin.** 1999. Nup124p is a nuclear pore factor of Schizosaccharomyces pombe that is important for nuclear import and activity of retrotransposon Tf1. Mol. Cell Biol. **19:**5768–5784.
4. **Ball, J. R., and K. S. Ullman.** 2005. Versatility at the nuclear pore complex: lessons learned from the nucleoporin Nup153. Chromosoma **114:**319–330.
5. **Bastos, R., A. Lin, M. Enarson, and B. Burke.** 1996. Targeting and function in mRNA export of nuclear pore complex protein Nup153. J. Cell Biol. **134:**1141–1156.
6. **Braaten, D., E. K. Franke, and J. Luban.** 1996. Cyclophilin A is required for the replication of group M human immunodeficiency virus type 1 (HIV-1) and simian immunodeficiency virus SIV(CPZ)GAB but not group O HIV-1 or other primate immunodeficiency viruses. J. Virol. **70:**4220–4227.
7. **Brass, A. L., et al.** 2008. Identification of host proteins required for HIV infection through a functional genomic screen. Science **319:**921–926.
8. **Brown, P. O., B. Bowerman, H. E. Varmus, and J. M. Bishop.** 1989. Retroviral integration: structure of the initial covalent product and its precursor, and a role for the viral IN protein. Proc. Natl. Acad. Sci. U. S. A. **86:**2525–2529.
9. **Butler, S. L., M. S. Hansen, and F. D. Bushman.** 2001. A quantitative assay for HIV DNA integration in vivo. Nat. Med. **7:**631–634.
10. **Chang, L. J., V. Urlacher, T. Iwakuma, Y. Cui, and J. Zucali.** 1999. Efficacy and safety analyses of a recombinant human immunodeficiency virus type 1 derived vector system. Gene Ther. **6:**715–728.
11. **Chatterji, U., et al.** 2009. The isomerase active site of cyclophilin A is critical for hepatitis C virus replication. J. Biol. Chem. **284:**16998–17005.
12. **Chen, C. M., et al.** 1999. Production and design of more effective avian replication-incompetent retroviral vectors. Dev. Biol. **214:**370–384.
13. **Christ, F., et al.** 2008. Transportin-SR2 imports HIV into the nucleus. Curr. Biol. **18:**1192–1202.
14. **Dang, V. D., and H. L. Levin.** 2000. Nuclear import of the retrotransposon Tf1 is governed by a nuclear localization signal that possesses a unique requirement for the FXFG nuclear pore factor Nup124p. Mol. Cell. Biol. **20:**7798–7812.
15. **Dar, M. J., et al.** 2009. Biochemical and virological analysis of the 18-residue C-terminal tail of HIV-1 integrase. Retrovirology **6:**94.
16. **Dismuke, D. J., and C. Aiken.** 2006. Evidence for a functional link between uncoating of the human immunodeficiency virus type 1 core and nuclear import of the viral preintegration complex. J. Virol. **80:**3712–3720.
17. **Ebina, H., J. Aoki, S. Hatta, T. Yoshida, and Y. Koyanagi.** 2004. Role of Nup98 in nuclear entry of human immunodeficiency virus type 1 cDNA. Microbes Infect. **6:**715–724.

18. **Engelman, A., I. Oztop, N. Vandegraaff, and N. K. Raghavendra.** 2009. Quantitative analysis of HIV-1 preintegration complexes. Methods **47:**283–290.
19. **Fassati, A., and S. P. Goff.** 2001. Characterization of intracellular reverse transcription complexes of human immunodeficiency virus type 1. J. Virol. **75:**3626–3635.
20. **Fassati, A., and S. P. Goff.** 1999. Characterization of intracellular reverse transcription complexes of Moloney murine leukemia virus. J. Virol. **73:**8919–8925.
21. **Forshey, B. M., U. von Schwedler, W. I. Sundquist, and C. Aiken.** 2002. Formation of a human immunodeficiency virus type 1 core of optimal stability is crucial for viral replication. J. Virol. **76:**5667–5677.
22. **Freed, E. O., G. Englund, and M. A. Martin.** 1995. Role of the basic domain of human immunodeficiency virus type 1 matrix in macrophage infection. J. Virol. **69:**3949–3954.
23. **Fujiwara, T., and K. Mizuuchi.** 1988. Retroviral DNA integration: structure of an integration intermediate. Cell **54:**497–504.
24. **Gallay, P., T. Hope, D. Chin, and D. Trono.** 1997. HIV-1 infection of nondividing cells through the recognition of integrase by the importin/karyopherin pathway. Proc. Natl. Acad. Sci. U. S. A. **94:**9825–9830.
25. **Ganser-Pornillos, B. K., U. K. von Schwedler, K. M. Stray, C. Aiken, and W. I. Sundquist.** 2004. Assembly properties of the human immunodeficiency virus type 1 CA protein. J. Virol. **78:**2545–2552.
26. **Guntaka, R. V., O. C. Richards, P. R. Shank, H. J. Kung, and N. Davidson.** 1976. Covalently closed circular DNA of avian sarcoma virus: purification from nuclei of infected quail tumor cells and measurement by electron microscopy and gel electrophoresis. J. Mol. Biol. **106:**337–357.
27. **Harborth, J., S. M. Elbashir, K. Bechert, T. Tuschl, and K. Weber.** 2001. Identification of essential genes in cultured mammalian cells using small interfering RNAs. J. Cell Sci. **114:**4557–4565.
28. **Hase, M. E., and V. C. Cordes.** 2003. Direct interaction with nup153 mediates binding of Tpr to the periphery of the nuclear pore complex. Mol. Biol. Cell **14:**1923–1940.
29. **Hatziioannou, T., D. Perez-Caballero, S. Cowan, and P. D. Bieniasz.** 2005. Cyclophilin interactions with incoming human immunodeficiency virus type 1 capsids with opposing effects on infectivity in human cells. J. Virol. **79:**176–183.
30. **Hazuda, D. J., et al.** 2000. Inhibitors of strand transfer that prevent integration and inhibit HIV-1 replication in cells. Science **287:**646–650.
31. **He, J., et al.** 1997. CCR3 and CCR5 are co-receptors for HIV-1 infection of microglia. Nature **385:**645–649.
32. **Hofmann, W., et al.** 1999. Species-specific, postentry barriers to primate immunodeficiency virus infection. J. Virol. **73:**10020–10028.
33. **Iordanskiy, S., R. Berro, M. Altieri, F. Kashanchi, and M. Bukrinsky.** 2006. Intracytoplasmic maturation of the human immunodeficiency virus type 1 reverse transcription complexes determines their capacity to integrate into chromatin. Retrovirology **3:**4.
34. **Julias, J. G., A. L. Ferris, P. L. Boyer, and S. H. Hughes.** 2001. Replication of phenotypically mixed human immunodeficiency virus type 1 virions containing catalytically active and catalytically inactive reverse transcriptase. J. Virol. **75:**6537–6546.
35. **Katz, R. A., J. G. Greger, P. Boimel, and A. M. Skalka.** 2003. Human immunodeficiency virus type 1 DNA nuclear import and integration are mitosis independent in cycling cells. J. Virol. **77:**13412–13417.
36. **Khare, et al.** 2008. Durable, safe, multi-gene lentiviral vector expression in feline trabecular meshwork. Mol. Ther. **16:**97–106.
37. **Kim, M. K., K. C. Claiborn, and H. L. Levin.** 2005. The long terminal repeat-containing retrotransposon Tf1 possesses amino acids in gag that regulate nuclear localization and particle formation. J. Virol. **79:**9540–9555.
38. **Koh, Y., H. Haim, and A. Engelman.** 2011. Identification and characterization of persistent intracellular human immunodeficiency virus type 1 integrase strand transfer inhibitor activity. Antimicrob. Agents Chemother. **55:**42–49.
39. **König, R., et al.** 2008. Global analysis of host-pathogen interactions that regulate early-stage HIV-1 replication. Cell **135:**49–60.
40. **Krishnan, L., et al.** 2010. The requirement for cellular transportin 3 (TNPO3 or TRN-SR2) during infection maps to human immunodeficiency virus type 1 capsid and not integrase. J. Virol. **84:**397–406.
41. **Lee, K., et al.** 2010. Flexible use of nuclear import pathways by HIV-1. Cell Host Microbe **7:**221–233.
42. **Lewis, P. F., and M. Emerman.** 1994. Passage through mitosis is required for oncoretroviruses but not for the human immunodeficiency virus. J. Virol. **68:**510–516.
43. **Li, L., et al.** 2001. Role of the non-homologous DNA end joining pathway in the early steps of retroviral infection. EMBO J. **20:**3272–3281.
44. **Li, Y., A. K. Kar, and J. Sodroski.** 2009. Target cell type-dependent modulation of human immunodeficiency virus type 1 capsid disassembly by cyclophilin A. J. Virol. **83:**10951–10962.
45. **Limón, A., N. Nakajima, R. Lu, H. Z. Ghory, and A. Engelman.** 2002. Wild-type levels of nuclear localization and human immunodeficiency virus type 1 replication in the absence of the central DNA flap. J. Virol. **76:**12078–12086.
46. **Loewen, N., et al.** 2003. FIV vectors. Methods Mol. Biol. **229:**251–271.
47. **Lu, R., et al.** 2004. Class II integrase mutants with changes in putative nuclear localization signals are primarily blocked at a postnuclear entry step of human immunodeficiency virus type 1 replication. J. Virol. **78:**12735–12746.
48. **Mackay, D. R., S. W. Elgort, and K. S. Ullman.** 2009. The nucleoporin Nup153 has separable roles in both early mitotic progression and the resolution of mitosis. Mol. Biol. Cell **20:**1652–1660.
49. **Mackay, D. R., M. Makise, and K. S. Ullman.** 2010. Defects in nuclear pore assembly lead to activation of an Aurora B-mediated abscission checkpoint. J. Cell Biol. **191:**923–931.
50. **Mattaj, I. W., and L. Englmeier.** 1998. Nucleocytoplasmic transport: the soluble phase. Annu. Rev. Biochem. **67:**265–306.
51. **McDonald, D., et al.** 2002. Visualization of the intracellular behavior of HIV in living cells. J. Cell Biol. **159:**441–452.
52. **Miller, M. D., C. M. Farnet, and F. D. Bushman.** 1997. Human immunodeficiency virus type 1 preintegration complexes: studies of organization and composition. J. Virol. **71:**5382–5390.
53. **Mörner, A., et al.** 1999. Primary human immunodeficiency virus type 2 (HIV-2) isolates, like HIV-1 isolates, frequently use CCR5 but show promiscuity in coreceptor usage. J. Virol. **73:**2343–2349.
54. **Nakajima, N., R. Lu, and A. Engelman.** 2001. Human immunodeficiency virus type 1 replication in the absence of integrase-mediated DNA recombination: definition of permissive and nonpermissive T-cell lines. J. Virol. **75:**7944–7955.
55. **Newman, R. M., et al.** 2006. Balancing selection and the evolution of functional polymorphism in Old World monkey TRIM5alpha. Proc. Natl. Acad. Sci. U. S. A. **103:**19134–19139.
56. **Olsen, J. C.** 1998. Gene transfer vectors derived from equine infectious anemia virus. Gene Ther. **5:**1481–1487.
57. **O'Rourke, J. P., G. C. Newbound, D. B. Kohn, J. C. Olsen, and B. A. Bunnell.** 2002. Comparison of gene transfer efficiencies and gene expression levels achieved with equine infectious anemia virus- and human immunodeficiency virus type 1-derived lentivirus vectors. J. Virol. **76:**1510–1515.
58. **Perron, M. J., et al.** 2004. TRIM5alpha mediates the postentry block to N-tropic murine leukemia viruses in human cells. Proc. Natl. Acad. Sci. U. S. A. **101:**11827–11832.
59. **Rabut, G., V. Doye, and J. Ellenberg.** 2004. Mapping the dynamic organization of the nuclear pore complex inside single living cells. Nat. Cell Biol. **6:**1114–1121.
60. **Rivière, L., J. L. Darlix, and A. Cimarelli.** 2010. Analysis of the viral elements required in the nuclear import of HIV-1 DNA. J. Virol. **84:**729–739.
61. **Roe, T., T. C. Reynolds, G. Yu, and P. O. Brown.** 1993. Integration of murine leukemia virus DNA depends on mitosis. EMBO J. **12:**2099–2108.
62. **Sabri, N., et al.** 2007. Distinct functions of the Drosophila Nup153 and Nup214 FG domains in nuclear protein transport. J. Cell Biol. **178:**557–565.
63. **Schmitz, A., et al.** 2010. Nucleoporin 153 arrests the nuclear import of hepatitis B virus capsids in the nuclear basket. PLoS Pathog. **6:**e1000741.
64. **Sokolskaja, E., D. M. Sayah, and J. Luban.** 2004. Target cell cyclophilin A modulates human immunodeficiency virus type 1 infectivity. J. Virol. **78:**12800–12808.
65. **Song, C., and C. Aiken.** 2007. Analysis of human cell heterokaryons demonstrates that target cell restriction of cyclosporine-resistant human immunodeficiency virus type 1 mutants is genetically dominant. J. Virol. **81:**11946–11956.
66. **Suzuki, Y., and R. Craigie.** 2007. The road to chromatin-nuclear entry of retroviruses. Nat. Rev. Microbiol. **5:**187–196.
67. **Thys, W., et al.** 2011. Interplay between HIV entry and transportin-SR2 dependency. Retrovirology **8:**7.
68. **Ulm, J. W., M. Perron, J. Sodroski, and C. M. R.** 2007. Complex determinants within the Moloney murine leukemia virus capsid modulate susceptibility of the virus to Fv1 and Ref1-mediated restriction. Virology **363:**245–255.
69. **Vaquerizas, J. M., et al.** 2010. Nuclear pore proteins nup153 and megator define transcriptionally active regions in the Drosophila genome. PLoS Genet. **6:**e1000846.
70. **Varadarajan, P., et al.** 2005. The functionally conserved nucleoporins Nup124p from fission yeast and the human Nup153 mediate nuclear import and activity of the Tf1 retrotransposon and HIV-1 Vpr. Mol. Biol. Cell **16:**1823–1838.
71. **Walther, T. C., et al.** 2001. The nucleoporin Nup153 is required for nuclear pore basket formation, nuclear pore complex anchoring and import of a subset of nuclear proteins. EMBO J. **20:**5703–5714.
72. **Willey, R. L., et al.** 1988. In vitro mutagenesis identifies a region within the envelope gene of the human immunodeficiency virus that is critical for infectivity. J. Virol. **62:**139–147.
73. **Woodward, C. L., S. Prakobwanakit, S. Mosessian, and S. A. Chow.** 2009. Integrase interacts with nucleoporin NUP153 to mediate the nuclear import of human immunodeficiency virus type 1. J. Virol. **83:**6522–6533.
74. **Wu, J., M. J. Matunis, D. Kraemer, G. Blobel, and E. Coutavas.** 1995. Nup358, a cytoplasmically exposed nucleoporin with peptide repeats, Ran-

GTP binding sites, zinc fingers, a cyclophilin A homologous domain, and a leucine-rich region. J. Biol. Chem. **270:**14209–14213.
75. **Yamashita, M., and M. Emerman.** 2004. Capsid is a dominant determinant of retrovirus infectivity in nondividing cells. J. Virol. **78:**5670–5678.
76. **Yamashita, M., and M. Emerman.** 2005. The cell cycle independence of HIV infections is not determined by known karyophilic viral elements. PLoS Pathog. **1:**e18.
77. **Yamashita, M., and M. Emerman.** 2006. Retroviral infection of non-dividing cells: old and new perspectives. Virology **344:**88–93.
78. **Yamashita, M., O. Perez, T. J. Hope, and M. Emerman.** 2007. Evidence for direct involvement of the capsid protein in HIV infection of nondividing cells. PLoS Pathog. **3:**1502–1510.
79. **Yan, N., P. Cherepanov, J. E. Daigle, A. Engelman, and J. Lieberman.** 2009. The SET complex acts as a barrier to autointegration of HIV-1. PLoS Pathog. **5:**e1000327.
80. **Yoo, S., et al.** 1997. Molecular recognition in the HIV-1 capsid/cyclophilin A complex. J. Mol. Biol. **269:**780–795.
81. **Zaitseva, L., et al.** 2009. HIV-1 exploits importin 7 to maximize nuclear import of its DNA genome. Retrovirology **6:**11.
82. **Zhang, F., T. Hatziioannou, D. Perez-Caballero, D. Derse, and P. D. Bieniasz.** 2006. Antiretroviral potential of human tripartite motif-5 and related proteins. Virology **353:**396–409.
83. **Zhang, R., R. Mehla, and A. Chauhan.** 2010. Perturbation of host nuclear membrane component RanBP2 impairs the nuclear import of human immunodeficiency virus-1 preintegration complex (DNA). PLoS One **5:**e15620.
84. **Zhou, H., et al.** 2008. Genome-scale RNAi screen for host factors required for HIV replication. Cell Host Microbe **4:**495–504.
85. **Zhou, L., and N. Pante.** 2010. The nucleoporin Nup153 maintains nuclear envelope architecture and is required for cell migration in tumor cells. FEBS Lett. **584:**3013–3020.